Inorg. Chem. **2007**, *46*, 9473–9480

Aerosol Assisted Chemical Vapor Deposition of In_2O_3 Films from Me_3In and Donor Functionalized Alcohols

Siama Basharat,[†] Claire J. Carmalt,*[,†] Sarah A. Barnett,[†] Derek A. Tocher,[†] and Hywel O. Davies[‡]

Materials Chemistry Centre, Department of Chemistry, University College London, 20 Gordon Street, London WC1H 0AJ, United Kingdom, and SAFC Epichem, Power Road, Bromborough, Wirral CH62 3QF, United Kingdom

Received July 10, 2007

The reaction of Me_3In and ROH (R = $CH_2CH_2NMe_2$, $CH(CH_3)CH_2NMe_2$, $C(CH_3)_2CH_2OMe$, CH_2CH_2OMe) in toluene under aerosol assisted chemical vapor deposition (AACVD) conditions leads to the production of indium oxide thin films on glass. The indium oxide films were deposited at 550 °C and analyzed by scanning electron microscopy (SEM), X-ray powder diffraction, wavelength dispersive analysis of X-rays (WDX), X-ray photoelectron spectroscopy (XPS), and Raman spectroscopy. This CVD technique offers a rapid, convenient route to In_2O_3, which presumably involves the in situ formation of dimethylindium alkoxides, of the type $[Me_2InOR]_2$. In order to identify compounds present in the aerosol mist, the solution-phase reaction between Me_3In and ROH (R = $CH_2CH_2NMe_2$, $C(CH_3)_2CH_2OMe$, $CH(CH_3)CH_2NMe_2$, $CH(CH_2NMe_2)_2$) at room temperature in toluene was carried out. Dimeric indium alkoxides, of the type $[Me_2In(OR)]_2$, were isolated, and their structures were determined by X-ray crystallography.

Introduction

Indium oxide thin films (doped and undoped) are attractive materials for use as transparent conductors, in applications such as display panels and solar cell windows.[1] Undoped indium oxide is used in industrial and technological applications such as toxic/dangerous gas detection in chemical plants due to both its transparency and conductivity.[2,3] Indium oxide can be doped with other metals to enhance its electronic properties; for example, tin-doped indium oxide (ITO) has an optical band gap of more than 3.4 eV.[4] ITO thin films are widely used in optoelectronic devices such as transparent electrodes for light emitting diodes,[5−9] flat panel displays,[10,11] and photovoltaic cells[12−14] due to their high transparency in the visible light region, low electric resistivity, chemical stability, and excellent adhesion to substrate.[15]

The production of thin films by chemical vapor deposition (CVD) affords inexpensive, adhesive, reproducible films with low impurity levels. However, In_2O_3 films are difficult to prepare by thermal CVD methods due to the lack of precursor materials with high vapor pressure and low decomposition temperatures. Thus, there have been few reports of dual source thermal CVD routes to In_2O_3, although polycrystalline indium oxide thin films have been deposited via plasma metal organic CVD or atmospheric pressure CVD of Me_3In and O_2.[16,17] A number of indium precursors have been investigated, including indium diketonate, carboxylate, alkyl,

* To whom correspondence should be addressed. Phone: +44 2076797528. Fax: +44 2076797463. E-mail: c.j.carmalt@ucl.ac.uk.
[†] University College London.
[‡] SAFC Epichem.

(1) Sharma, S.; Sunkara, M. K. *J. Am. Chem. Soc*. **2002**, *124*, 12288.
(2) Avaritsiotis, J. N.; Howson, R. P. *Thin Solid Films* **1980**, *80*, 63.
(3) Weiher, R. L.; Ley, R. P. *J. Appl. Phys.* **1966**, *37*, 299.
(4) Muller, H. K. *Phys. Status Solid* **1969**, *27*, 723.
(5) Xirouchaki, C.; Kiriakidis, G.; Pedersen, T. F.; Fritzsche, H. *J. Appl. Phys.* **1996**, *79*, 9349.
(6) Tang, C. W.; Van Slyke, S. A. *Appl. Phys. Lett*. **1987**, *51*, 913.
(7) Burroughes, J. H.; Bradley, D. D. C.; Brown, A. R.; Marks, R. N.; Mackay, K.; Friend, R. H.; Burns, P. L.; Holmes, A. B. *Nature* **1990**, *347*, 539.
(8) Sheats, J. R.; Antoniadis, H.; Hueschen, M.; Leonard, W.; Miller, J.; Moon, R.; Roitman, D.; Stocking, A. *Science* **1996**, *273*, 884.
(9) Leger, J. M.; Carter, S. A.; Ruhstaller, B.; Nothofer, H.-G.; Scherf, U.; Tillman, H.; Horhold, H.-H. *Phys. Rev. B* **2003**, *68*, 054209.
(10) Hsu, S.-F.; Lee, C.-C.; Hwang, S.-W.; Chen, C. H. *Appl. Phys. Lett.* **2005**, *86*, 253508.
(11) Lee, B. H.; Kim, I. G.; Cho, S. W.; Lee, S. H. *Thin Solid Films* **1997**, *302*, 25.
(12) Tahar, R. B. H.; Ban, T.; Ohaya, T.; Takahashi, Y. *J. Appl. Phys.* **1998**, *83*, 2631.
(13) Breeze, A. J.; Schlesinger, Z.; Carter, S. A.; Brock, P. J. *Phys. Rev. B* **2001**, *64*, 125205.
(14) Zhang, F.; Johansson, M.; Anderson, M. R.; Hummelen, J. C.; Inganas, O. *Adv. Mater*. **2002**, *14*, 662.
(15) Kymakis, E.; Amaratunga, G. A. J. *Appl. Phys. Lett*. **2002**, *80*, 112.
(16) Maruyama, T.; Kitamura, T. *Jpn. J. Appl. Phys.* **1989**, *28*, L1096.
(17) Murphy, S. D.; Langlois, E.; Bhat, L.; Gutmann, R.; Brown, E.; Dzeindziel, R.; Freeman, M.; Choudry, N. *AIP Conf. Proc*. **1996**, *358*, 290.

10.1021/ic701372b CCC: $37.00
Published on Web 10/03/2007

hydroxide, and halide complexes; however, none of these precursors are entirely satisfactory.[18−21] Indium diketonate and carboxylate complexes, for example, are solids at moderate temperatures, a property that can produce variable precursor delivery to the substrate. Recently, the formation of In_2O_3 films from $[In(\mu\text{-}OCMe_2Et)(OCMe_2Et)_2]_2$,[21] $[In(OCMe(CF_3)_2)_3(H_2N^tBu)]$,[22] and $[Me_2In(OC(CF_3)_2CH_2NHMe)]$[2,23] in the presence of O_2 as the reactive carrier gas, via low pressure (LP)CVD, has been reported. However, the presence of fluorine in the precursors could result in fluorine contamination in the resulting In_2O_3 films.

This paper represents the first thin film growth of indium oxide by a novel aerosol assisted (AA)CVD route to In_2O_3 from the reaction of Me_3In and donor functionalized alcohols. AACVD uses a liquid−gas aerosol to transport soluble precursors to a heated substrate and is a useful method when a conventional atmospheric pressure CVD precursor proves involatile or thermally unstable. By designing precursors specifically for AACVD, the restrictions of volatility and thermal stability are lifted, and new precursors and films can be investigated. Different and unique morphologies of films can be obtained by AACVD due to the influence of the solvent on the deposition, which could potentially lead to improved properties. Furthermore, thin films can be deposited under AACVD conditions at low temperatures and require only minimal amounts of precursor (ca. 0.1 g). In this study, indium alkoxides were generated in situ from the reaction of Me_3In and ROH ($R = CH_2CH_2NMe_2$, $CH(CH_3)CH_2NMe_2$, $C(CH_3)_2CH_2OMe$, CH_2CH_2OMe) in toluene. An aerosol of this reaction mixture was then passed over a heated glass substrate, which resulted in the deposition of thin films of indium oxide. These ligands were chosen for AACVD, as they lead to precursors, which are less air/moisture sensitive and have increased solubility.[24] Thus, the high moisture sensitivity of dialkylindium alkoxides makes them difficult to use in solution-based CVD. Therefore, modified alkoxides, such as the donor functionalized ligands ($OCH_2CH_2NMe_2$, $CH(CH_3)CH_2NMe_2$ etc), which have an increased coordinative saturation at the metal center, have been used as alternatives to $[Me_2InOR']$ ($R' =$ alkyl or aryl) in AACVD. The aminoalkoxide ligands also eliminate the necessity of introducing an extra donor group to stabilize the electron deficient indium alkoxide complex. The synthesis and crystal structures of indium mono(alkoxides), of the type $[Me_2In(OR)]_2$, prepared from the solution-phase reaction of Me_3In and ROH, are also reported.

Experimental Section

General Procedures - AACVD. Nitrogen (99.99%) was obtained from BOC and used as supplied. Depositions were obtained on SiCO coated float-glass. Prior to use the glass substrates were cleaned using petroleum ether (60−80 °C) and propan-2-ol and then dried in air. Glass substrates of ca. 90 mm × 45 mm × 4 mm were used. The precursor was dissolved in solvent and vaporized at room temperature by use of a PIFCO ultrasonic humidifier. This produced an aerosol of the precursor in the solvent used. Two-way taps were used to divert the nitrogen carrier gas through the bubbler. The aerosol was carried into the reactor in a stream of nitrogen gas through a brass baffle to obtain a laminar flow.

A graphite block containing a Whatman cartridge heater was used to heat the glass substrate. The temperature of the substrate was monitored by a Pt−Rh thermocouple. Depositions were carried out by heating the horizontal bed reactor to the required temperature before diverting the nitrogen line through the aerosol and hence to the reactor. The total time for the deposition process was in the region of 2−3 h. At the end of the deposition the nitrogen flow through the aerosol was diverted, and only nitrogen passed over the substrate. The glass substrate was allowed to cool with the graphite block to less than 100 °C before it was removed. Coated substrates were handled and stored in air. Large pieces of glass (ca. 4 cm × 2 cm) were used for X-ray powder diffraction. The coated glass substrate was cut into ca. 1 cm × 1 cm squares for subsequent analysis by SEM, WDX, XPS, transmission/reflectance, and UV absorption studies.

Film Analysis Methods. X-ray powder diffraction patterns were measured on a Siemens D5000 diffractometer using monochromated $CuK_{\alpha 1}$ radiation ($\lambda = 1.5400$ Å). The diffractometer used glancing incident radiation (1.5°). The films on the glass substrates were indexed using Unit Cell and compared to database standards. Raman spectra were acquired using a Renishaw Raman system 1000 using a helium-neon laser of wavelength 632.8 nm. The Raman system was calibrated against the emission lines of neon. SEM was carried out on a JEOL 6301 filament scanning electron microscope, and WDX was obtained on a Philips XL30SEM instrument. X-ray photoelectron spectra were recorded using a VG ESCALAB 220i XL instrument using focused (300 μm spot) monochromatic Al Kα radiation at a pass energy of 20 eV. Scans were acquired with steps of 50 meV. A flood gun was used to control charging, and binding energies were referred to an adventitious C 1s peak at 285.0 eV. Reflectance and transmission spectra were recorded between 300 and 1000 nm by a Zeiss miniature spectrometer. Reflectance measurements were standardized relative to a rhodium mirror and transmission relative to air. UV−vis spectra were recorded using a Helios double beam instrument between 200 and 1000 nm.

General Procedures - Synthesis. All manipulations were performed under a dry, oxygen-free dinitrogen atmosphere using standard Schlenk techniques or in an Mbraun Unilab glovebox. All solvents used were stored in alumina columns and dried with anhydrous engineering equipment, such that the water concentration was 5−10 ppm. SAFC HiTech supplied trimethylindium. All other reagents were procured commercially from Aldrich, and the alcohols were degassed by three freeze−pump−thaw cycles and stored over 4 Å molecular sieves. Microanalytical data were obtained at University College London

All ^1H and ^{13}C NMR spectra were obtained on a Bruker AMX400 spectrometer, operating at 400.12 MHz. All spectra were recorded using C_6D_6, which was dried and degassed over molecular sieves prior to use; ^1H and ^{13}C chemical shifts are reported relative to $SiMe_4$ (δ 0.00). All IR spectra were recorded using a Shimadzu

(18) Lobinger, P.; Park, H. S.; Hohmeister, H.; Roesky, H. W. *Chem. Vap. Deposition* **2001**, *3*, 7.
(19) Wang, A.; Dai, J.; Cheng, J.; Chudzik, M. P.; Marks, T. J.; Chang, R. P. H.; Kannewurf, C. R. *Appl. Phys. Lett.* **1998**, *73*, 327.
(20) Maruyama, T.; Fukui, K. *J. Appl. Phys.* **1991**, *70*, 3848.
(21) Suh, S.; Hoffman, D. M. *J. Am. Chem. Soc*. **2000**, *122*, 9396 and references therein.
(22) Mîinea, L.; Suh, S.; Hoffman, D. M. *Inorg. Chem.* **1999**, *38*, 4447.
(23) Chou, T.-Y.; Chi, Y.; Huang, S.-F.; Liu, C.-S.; Carty, A. J.; Scoles, L.; Udachin, K. A. *Inorg. Chem*. **2003**, *42*, 6041.
(24) Basharat, S.; Carmalt, C. J.; King, S. J.; Peters, E. S.; Tocher, D. A. *Dalton Trans.* **2004**, 3475−3480.

Table 1. X-ray Structural Data of Complexes for **1**−**4**[a]

	1	**2**	**3**	**4**
formula	$C_6H_{16}InNO$	$C_{14}H_{36}In_2N_2O_2$	$C_7H_{17}InO_2$	$C_9H_{23}InN_2O$
formula weight	233.02	494.09	248.03	289.11
T	150(2) K	150(2) K	150(2) K	150(2) K
crystal system	orthorhombic	monoclinic	monoclinic	triclinic
space group	*Pccn*	$P2_1/n$	$P2_1/n$	$P\bar{1}$
a (Å)	11.6733(14)	15.5563(12)	8.3096(9)	8.3820(8)
b (Å)	15.6152(18)	8.1075(6)	15.0739(16)	8.4014(8)
c (Å)	10.3060(12)	16.7231(13)	8.7685(9)	10.1223(10)
α (deg)	90	90	90	66.1840(10)
β (deg)	90	96.9500(10)	112.743(2)	85.316(2)
γ (deg)	90	90	90	82.575(2)
V (Å^3)	1878.6(4)	2093.7(3)	1012.93(19)	646.31(11)
Z	8	4	4	2
D_c (g/cm^3)	1.648	1.567	1.626	1.491
μ(MoKα) mm^{-1}	2.453	2.206	2.285	1.801
reflns collected	10284	17802	5818	5495
indep reflns (R_{int})	2265(0.0188)	4977(0.0149)	2235(0.0155)	2915(0.0137)
R_1 [$1 > 2\sigma(I)$][b]	0.0201	0.0183	0.0180	0.0243
wR_2 (all data)[c]	0.0466	0.0431	0.0427	0.0610

[a] Bruker SMART APEX diffractometer ω rotation with narrow frames, graphite monochromated Mo Kα radiation, refinement based on F^2. [b] $R_1 = \Sigma||F_o| - |F_c||/\Sigma|F_o|$. [c] $wR_2 = \{\Sigma[w(F_o^2 - F_c^2)^2]/\Sigma[w(F_o^2)^2]\}^{1/2}$; $w^{-1} = \sigma^2(F_o^2) + (aP)^2 + bP$.

FTIR-8200 spectrometer, operating in the region of 4000−400 cm^{-1}. The IR samples were prepared using nujol. The mass spectra were obtained using a Micromass 70-SE spectrometer using chemical ionization (CI) with methane reagent gas.

AACVD Reaction of Me_3In and $HOCH_2CH_2NMe_2$. $HOCH_2CH_2NMe_2$ (1.89 mL, 18.8 mmol) was placed in 30 mL of toluene in the AACVD bubbler and used to pretreat the reactor for 5 min before the addition of Me_3In. After pretreating the reactor, Me_3In (0.5 g, 3.13 mmol) was added to the bubbler. The mixture was allowed to react for 60 min prior to deposition.

AACVD Reaction of Me_3In and $HOCH(CH_3)CH_2NMe_2$. The procedure was the same as above but using $HOCH(CH_3)CH_2NMe_2$ (2.22 mL, 18.8 mmol).

AACVD Reaction of Me_3In and $HOC(CH_3)_2CH_2OMe$. The procedure was the same as above but using $HOC(CH_3)_2CH_2OMe$ (2.17 mL, 18.8 mmol).

AACVD Reaction of Me_3In and $HOCH_2CH_2OMe$. The procedure was the same as above but using $HOCH_2CH_2OMe$ (1.48 mL, 18.8 mmol).

Synthesis of $[Me_2In(OCH_2CH_2NMe_2)]_2$ (1). $HOCH_2CH_2NMe_2$ (0.98 mL, 9.80 mmol) was added dropwise to a solution of Me_3In (1.57 g, 9.80 mmol) in toluene (20 mL) at −78 °C with stirring over a 0.5 h period. The reaction mixture was allowed to warm slowly to room temperature and stirred for a further 24 h. Removal of the solvent in vacuo afforded a caked white solid. The solid was redissolved in toluene (2 mL) and cooled to −20 °C. Compound **1** was obtained as a white microcrystalline solid after several days (1.86 g, yield 58%). Anal. Calc. for $C_6H_{16}ONIn$: C, 30.93; H, 6.92; N, 6.01. Found: C, 30.45; H, 6.17; N, 5.80. ^{1}H NMR δ/ppm (C_6D_6): 0.04 (s, *Me*$_2$In, 3H), 2.99 (s, NC*H*$_3$, 6H), 3.89 (t, OCH$_2$C*H*$_2$N, 2H, J = 5.4 Hz), 4.13 (t, OC*H*$_2$CH$_2$N, 2H, J = 5.40 Hz). ^{13}C{^{1}H}NMR δ/ppm (C_6D_6): −8.5 (Me_2In), 44.5 (N*C*H$_3$), 58.1 (OCH$_2$*C*H$_2$N), 62.9 (O*C*H$_2$). IR (cm^{-1}): 2921 vs, 2694 w, 2271 m, 2206 m, 1990 vs, 1730 vs, 1660 vs, 1624 vs, 1455 s, 1406 m, 1377 m, 1353 s, 1275 m, 1261 m, 1184 w, 1168 w, 1150 s, 1096 vs, 1028 m, 947 s, 888 s, 783 s, 695 vs, 603 vs mass spec. (CI): (*m*/*z*) 642 ([M]$_2$), 556 ([M]$_2$ − OR), 320 ([M]), 234 ([M] − OR), 145 (Me_2In), 115 In and 90 $OCH_2CH_2NMe_2$.

Synthesis of $[Me_2In(OCH(CH_3)CH_2NMe_2)]_2$ (2). Compound **2** was prepared in the same manner as **1** but using $HOCH(CH_3)CH_2NMe_2$ (1.2 mL, 9.80 mmol) and Me_3In (1.57 g, 9.80 mmol) in toluene (20 mL). Removal of the solvent in vacuo afforded a yellow nonviscous oil. The reaction flask was left at room temperature, and X-ray quality crystals were obtained after 24 h (1.97 g, yield 41%). Anal. Calc. for $C_7H_{18}NOIn$: C, 34.17; H, 6.96; N, 5.69. Found: C, 34.07; H, 6.66; N, 5.03. ^{1}H NMR δ/ppm (C_6D_6): δ 0.00 (s, Me_2In, 6H), 1.56 (d, OCH(C*H*$_3$), 3H, J = 6.10 Hz), 1.90 (s, NC*H*$_3$, 6H), 2.08 (t, OCHC*H*$_2$N, 2H, J = 11.1 Hz), 3.81 (m, OC*H*(CH$_3$)CH$_2$, 1H). ^{13}C{^{1}H} NMR δ/ppm (C_6D_6): δ −4.6 (Me_2In), 24.1 (OCH(*C*H$_3$)), 46.6 (N*C*H$_3$), 65.2 (OCH*C*H$_2$N), 69.2 (O*C*H). IR (cm^{-1}): 2923 s, 2728 m, 2599 m, 2276 m, 1624 s, 1456 m, 1366 w, 1337 w, 1313 w, 1280 m, 1195 w, 1138 m, 1089 m, 1024 s, 946 s, 863 w, 835 w, 801 vs, 695 vs, 666 m, 588 vs Mass spec. (CI): (*m*/*z*) 493 ([M]$_2$), 479 [M] − Me, 392 ([M] − MeIn), 248 (Me_2In − $OCH(CH_3)CH_2NMe_2$), 232 (MeIn($OCH(CH_3)CH_2NMe_2$)), 145 (Me_2In), 104 ($OCH(CH_3)CH_2NMe_2$).

Synthesis of $[Me_2In(OC(CH_3)_2CH_2OMe)]_2$ (3). Compound **3** was prepared in the same manner as **1** but using $HOC(CH_3)_2CH_2OMe$ (1.10 mL, 9.80 mmol) and Me_3In (1.57 g, 9.80 mmol) in toluene (20 mL). Removal of the solvent in vacuo afforded a caked white solid. The solid was redissolved in toluene (2 mL) and cooled to −20 °C. Compound **3** was obtained as a white microcrystalline solid after several days (1.25 g, yield 51%). Anal. Calc. for $C_7H_{17}O_2In$: C, 33.90; H, 6.91. Found: C, 33.19; H, 6.84. ^{1}H NMR δ/ppm (C_6D_6): 0.00 (s, Me_2In, 6H), 1.22 (s, OC(C*H*$_3$), 6H), 2.74 (s, OCC*H*$_2$, 2H), 2.90 (s, (O*Me*, 3H). ^{13}C{^{1}H} NMR δ/ppm (C_6D_6): −3.94 (Me_2In), 28.6 (OC(*C*H$_3$)), 57.6 (O*Me*), 70.6 (O*C*CH$_2$), 82.7 (OC*C*H$_2$). IR (cm^{-1}): 2917 vs, 2279 m, 2185 m, 2032 s, 1924 s, 1732 vs, 1665 vs, 1631 vs, 1454 vs, 1377 vs, 1262 s, 1231 s, 1176 s, 1155 vs, 1103 vs, 1022 s, 996 s, 961 s. 912 s, 793 s, 704 s, 612 s, 514 s. Mass spec. (CI): (*m*/*z*) 481 ([M]), 393 ([M] − $OC(CH_3)_2CH_2OMe$), 145 (Me_2In).

Synthesis of $[Me_2In(OCH(CH_2NMe_2)_2)]_2$ (4). Compound **4** was prepared in the same manner as **4** using $HOCH(CH_2NMe_2)_2$ (1.60 mL, 9.80 mmol) and Me_3In (1.57 g, 9.80 mmol) in toluene (20 mL). Removal of the solvent in vacuo afforded a pale yellow nonviscous oil. The reaction flask was left at room temperature, and X-ray quality crystals were obtained after 24 h (1.94 g, 69% yield). Anal. Calc. for $C_9H_{23}N_2OIn$: C, 37.39; H, 7.67; N, 9.69. Found: C, 37.29; H, 8.26; N, 8.90. ^{1}H NMR δ/ppm (C_6D_6): δ 0.01 (s, Me_2In, 6H), 1.89 (dd, OCHC*H*$_2$N, 2H, J = 3.1 Hz), 2.02 (s, NC*H*$_3$, 12H), 2.16 (m, OCHC*H*$_2$N, 2H), 3.80 (m, OCH, 1H). ^{13}C{^{1}H} NMR δ/ppm (C_6D_6): δ −5.3 (Me_2In), 46.1 (N*C*H$_3$), 64.3 (OCH*C*H$_2$N), 67.3 (O*C*H). IR (cm^{-1}): 2993 vs, 2854 vs, 2728 s,

Table 2. Analytical Data for the Deposition of In_2O_3 Thin Films by AACVD

oxygen precursor	In:O ratio from WDX	lattice constant, *a* (Å)
$HOCH_2CH_2NMe_2$	1:1.5	10.03
$HOCH(CH_3)CH_2NMe_2$	1:1.5	10.11
$HOC(CH_3)_2CH_2OMe$	1:1.4	10.03
$HOCH_2CH_2OMe$	1:1.3	10.03

2599 s, 2275 s, 1624 vs, 1455 m, 1366 m, 1337 w, 1312 w, 1280 m, 1257 m, 1195 m, 1138 s, 1089 s, 1024 s, 945 s, 863 m, 835 m, 801 s, 695 vs, 666 s, 588 s. Mass spec. (CI): (*m*/*z*) 435 ([M] − Me_2In), 291 ($Me_2In(OCH(CH_3)CH_2NMe_2)$, 275 ($MeIn(OCH(CH_3)CH_2NMe_2)$), 145 ($Me_2In$).

Crystal Structures Determination and Refinement. Crystals of **1** and **3** were isolated from toluene at −20 °C; crystals of **2** and **4** were obtained from oils at room temperature after a few days. A single crystal was mounted on a glass fiber, and all geometric and intensity data were taken from this sample on a Bruker SMART APEX CCD diffractometer using graphite-monochromated Mo Kα radiation (λ = 0.71073 Å) at 150 ± 2 K. Data reduction and integration were carried out with SAINT+,[25] and absorption corrections were applied using the program SADABS.[26] The structure was solved by direct methods using SHELXS-97[27] and developed using alternating cycles of least-squares refinement and difference Fourier synthesis.[28] All non-hydrogen atoms were refined anisotropically. Hydrogen atoms were placed in calculated positions, and their thermal parameters were linked to those of the atoms to which they were attached (riding model). Crystallographic refinement parameters of complexes **1**−**4** are summarized in Table 1, and the selected bond distances and angles of these complexes are listed in Table 3, respectively.

Results and Discussion

Aerosol Assisted Chemical Vapor Deposition. Brown/rainbow colored films have been deposited on glass from the dual-source AACVD reaction of Me_3In and ROH (R = $CH_2CH_2NMe_2$, $CH(CH_3)CH_2NMe_2$, $C(CH_3)_2CH_2OMe$, CH_2CH_2OMe) at 550 °C (Scheme 1). The reaction of Me_3In and excess ROH in toluene was assumed to generate in situ the dialkylindium mono(alkoxide), $[Me_2In(OR)]_2$ (vida infra).

Scheme 1. Solution Phase and AACVD Reactions of Me_3In and Donor Functionalized Alcohols

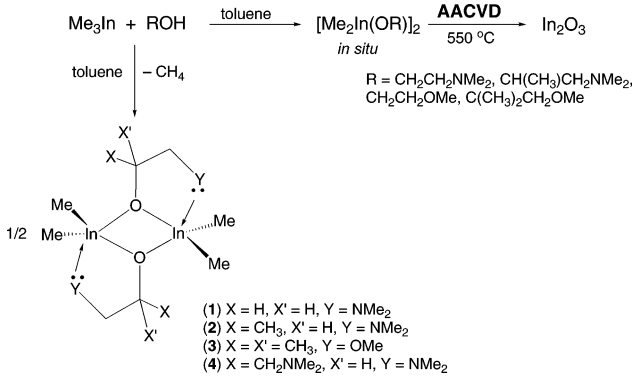

Deposition was observed on both the top plate and the substrate, which is consistent with the precursor decomposing on the substrate and the reactive species desorbing from the surface. The top plate was measured to be 50−75 °C lower in temperature than the substrate. The films deposited were uniform and covered the substrate completely. The films were adherent to the substrate, passing the Scotch tape test but readily scratched by a brass or stainless steel stylus.

The indium oxide films were characterized using a range of techniques. WDX analysis showed the films to have a metal-to-oxygen ratio close to the expected 1:1.5 for In_2O_3 (Table 2). The deviations from the In_2O_3 stoichiometry occurred when using $HOC(CH_3)_2CH_2OMe$ and $HOCH_2CH_2OMe_2$ where thinner films resulted in breakthrough to the underlying glass inhibiting accurate compositional analysis.

XPS of selected indium oxide films show binding energy shifts of 444.5 and 452.1 eV for $In3d_{5/2}$ and $In3d_{3/2}$, respectively. These values are in close agreement with literature values previously reported for In_2O_3.[29] XPS also showed a shift at 530.1 eV for the O 1s peak, which is in agreement with the literature value of 530.5 eV for O 1s in In_2O_3.[29] No evidence for carbon or nitrogen (for films grown

Table 3. Selected Bond Lengths (Å) and Angles (deg) for Complexes **1**−**4**

		2			
compd[a]	**1**	molecule A	molecule B	**3**	**4**
In−O	2.1432(14)	2.1342(12)	2.1342(12)	2.1433(13)	2.1894(18)
In−O′	2.2358(14)	2.2482(11)	2.2560(12)	2.2083(12)	2.1960(18)
In−L[b]	2.5161(16)	2.5376(15)	2.5641(15)	2.5810(13)	2.8329(21)
					2.9302(18)
In−C	2.1563(18)	2.1537(19)	2.1551(18)	2.154(2)	2.141(3)
	2.1555(18)	2.157(2)	2.150(2)	2.146(2)	2.154(3)
O−In−O′	71.75(6)	72.76(5)	73.53(5)	74.17(5)	72.76(7)
O−In−C	109.61(7)	114.42(8)	114.11(7)	111.04(7)	104.35(10)
	116.33(7)	112.24(8)	110.05(7)	113.75(8)	104.80(11)
O′−In−C	96.98(8)	96.98(7)	97.97(7)	103.54(7)	103.11(10)
	99.35(8)	98.34(8)	97.61(6)	103.99(7)	102.87(11)
C−In−C	133.99(9)	133.30(10)	135.70(8)	132.14(9)	145.48(14)
L−In−C	94.35(8)	96.43(8)	94.37(7)	91.31(7)	85.74 (av)
	96.90(8)	94.80(7)	94.58(7)	89.25(7)	
O−In−L	72.66(5)	73.33(5)	73.48(5)	69.27(4)	67.52
					68.81
O′−In−L	144.08(5)	146.02(5)	146.99(4)	143.37(4)	140.28
					141.56
In−O−In	108.25(6)	107.24(5)	106.47(5)	105.83(5)	107.24(7)

[a] Symmetry codes for O′: [a] $-x+1,-y+1,-z+1$; [b] $-x+1,-y+2,-z$; [c] $-x+1,-y,-z+2$; [d] $-x+1,-y,-z+1$. [b] L = N for **1**, **2**, and **4**; L = O for **3**.

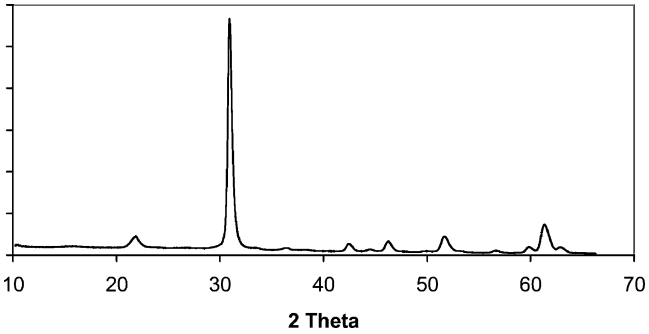

Figure 1. XRD pattern obtained for a In_2O_3 film deposited by AACVD from the in situ reaction of Me_3In and $HOCH_2CH_2OMe$ at 550 °C.

from $HOCH_2CH_2NMe_2$ and $HOCH(CH_3)CH_2NMe_2$) contamination was seen to the detection limits of the instrument.

All the films deposited were composed of cubic crystalline In_2O_3, and the XRD patterns showed strong reflections from the (222) plane. A representative powder XRD of all In_2O_3 films is shown in Figure 1. The In_2O_3 films showed only the formation of a single phase cubic In_2O_3. In general, indium oxide films are polycrystalline with a cubic structure in the bulk material, although a preferred orientation along the (222) plane is common.[18] The lattice constants were determined for the cubic-In_2O_3 films obtained, as summarized in Figure 2. These values were found to be close to the anticipated value for bulk In_2O_3 (a = 10.118 Å).[30] The Raman pattern obtained for the In_2O_3 films formed is characteristic of In_2O_3 and matches well with those previously reported.[31] The strongest band observed was broad at 363 cm^{-1} (with weaker bands at 304, 489, and 630 cm^{-1}).

The film morphology was studied using SEM, which indicated a needlelike morphology in most cases. This morphology is characteristic of an island growth mechanism. The needles are in the range of 4−10 μm in length, as shown in Figure 2. The SEM of the films deposited from Me_3In and $HOCH(CH_3)CH_2NMe_2$ suggests the formation of two different materials, spherical particles and needles. This could be due to the thickness of the film or the presence of a crystalline and amorphous material, although all analytical data suggest only the formation of In_2O_3. The SEM image for the film deposited from the reaction of Me_3In and $HOCH_2CH_2NMe_2$ shows a slightly different morphology, that of spherical particles. As commented in the Introduction, AACVD can result in different morphologies due to the effects of the solvent. It is also possible that changing the R group on the alcohol could result in a change in morphology. The films were between 0.4 and 0.8 μm thick, determined using cross-sectional SEM.

The optical properties of the films were studied by transmission, reflectance, and UV/visible measurements between 300 and 2500 nm. All films showed a slight shift in the adsorption edge toward the visible relative to a plain glass substrate. The indium oxide films displayed minimal reflectivity (5−10%) and high transmission (80−90%). Conducting a Tauc plot[32] of the UV/visible data indicated that the films had band gaps ranging from 3.5−3.7 eV. This is in agreement with values previously reported (3.75 eV).[33] The films were shown to have contact angles for water droplets of 28°, suggesting that the films are hydrophilic. However, the contact angles for these films did not change upon photoirradiation suggesting that this low contact angle is not due to some form of photoinduced hydrophilicity. The porosity of the films could be responsible for this hydrophilic character.

The successful formation of In_2O_3 thin films from the in situ AACVD reaction of Me_3In and ROH indicates that there is no need to prepare, isolate, and purify a single-source precursor. Crystalline cubic-In_2O_3 films were obtained from the AACVD reaction of Me_3In and ROH without the use of O_2 as a reactive carrier gas. Thus, the use of excess alcohol led to uniform In_2O_3 films with low levels of carbon contamination. The mechanism for the deposition process was not investigated. However, it is assumed to proceed to via decomposition processes reported previously for related systems.[34] The R group from $[Me_2InOR]_2$ is probably eliminated via β-hydride elimination when these complexes are pyrolyzed on or near the surface. The result of this would be the formation of intramolecular In−O bonds leading eventually to growth of In_2O_3. The mechanism for the decomposition of Me−In groups is likely to be based on the elimination of methyl radicals.

Synthesis. In order to gain an insight into compounds present in the aerosol mist of the AACVD reactions described above, the reaction of Me_3In and 1 equiv of ROH was carried out in toluene. In a typical synthesis, the donor-functionalized alcohol was added to Me_3In in toluene, resulting in a violent evolution of methane gas (Scheme 1). After workup, white solids (**1** and **3**) or colorless oils (**2** and **4**) resulted from which X-ray quality colorless crystals of compounds **1**−**4** were afforded in 41−68% yields. Analytical and spectroscopic data for **1**−**4** indicated that the dimeric complexes $[Me_2In(OR)]_2$ (R = $CH_2CH_2NMe_2$ (**1**), $CH(CH_3)CH_2NMe_2$ (**2**), $C(CH_3)_2CH_2OMe$ (**3**), and $CH(CHNMe_2)_2$ (**4**)) had been isolated. The reaction of R_3In with $HOCH_2CH_2NMe_2$ has been previously reported to yield the complex $[R_2In(OCH_2CH_2NMe_2)]_2$ (R = Me, Et).[35]

The dimeric nature of **1**−**4** was confirmed by single-crystal X-ray crystallography (Figures 4−7). Selected bond lengths and angles are given in Table 3. The centrosymmetric, four-membered In_2O_2 ring, that is common to this type of

(25) *Area detector control and data integration and reduction software*; Bruker AXS: Madison, WI, U.S.A., 2001.
(26) Sheldrick, G. M. *SADABS*; University of Göttingen: Germany, 1997.
(27) Sheldrick, G. M. *SHELXS-97*; University of Göttingen: Germany, 1997.
(28) Sheldrick, G. M. *SHELXL-97*; University of Göttingen: Germany, 1997.
(29) *Practical Surface Analysis*, 2nd ed.; Briggs, D., Seah, M. P., Eds.; Volume Auger and X-ray Photoelectron Spectroscopy, Wiley: New York, 1990.
(30) *JCPDS le 06-0416*; International Centre for Diffraction Data: Swarthmore, PA.
(31) Korotcenkova, G.; Brinzaria, V.; Ivanova, M.; Cerneavschia, A.; Rodriguezb, J.; Cirerab, A.; Cornetb, A.; Morante, J. *Thin Solid Films* **2005**, *479*, 38.
(32) *Proceedings of the International School of Physics*; Tauc, J., Ed.; Enrico Fermi, Course XXXIV, The Optical Properties of Solids, 1966.
(33) Passlack, J. *Appl. Phys.* **1995**, *77*, 686.
(34) Carmalt, C. J.; Basharat, S. *Precursors to Semiconducting Materials*; O'Hare, D., Ed.; Comprehensive Organometallic Chemistry III, 2007; Vol. 12, p 1.
(35) Maeda, T.; Okawara, R. *J. Organomet. Chem.* **1972**, *39*, 87.

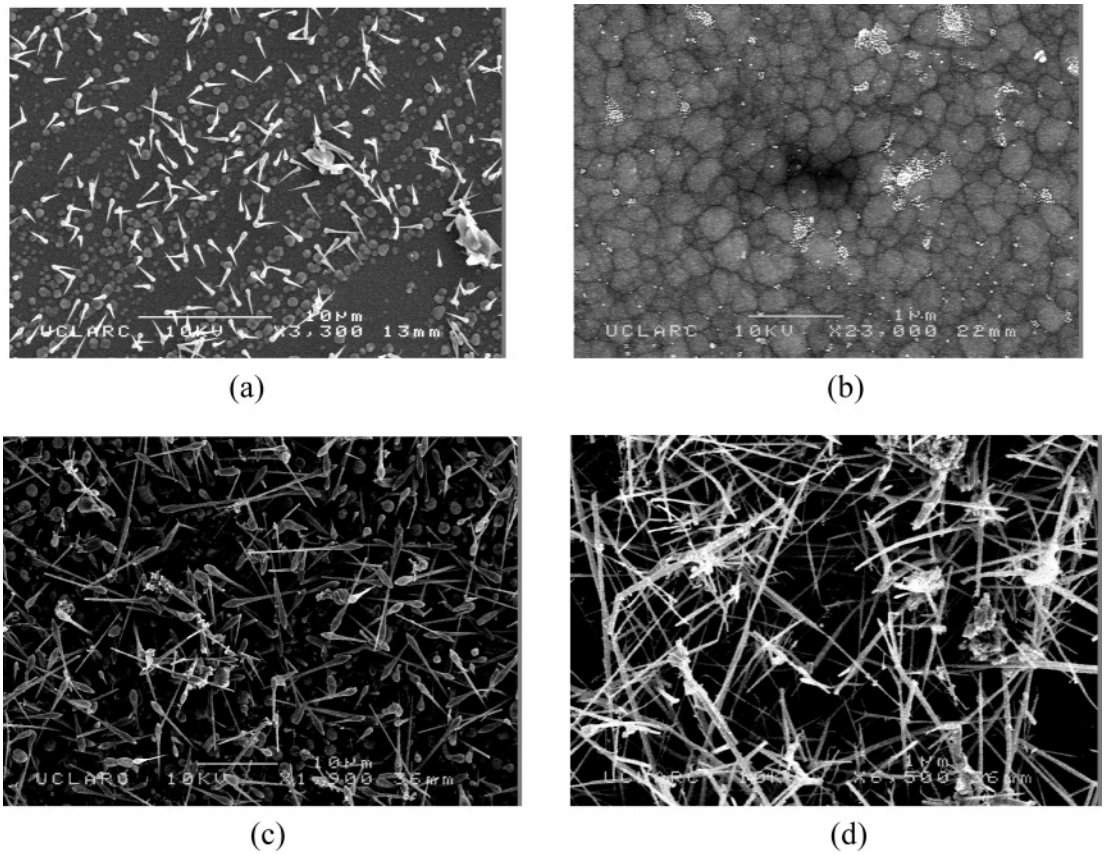

Figure 2. SEM images for In_2O_3 films deposited from the reaction of Me_3In and (a) $HOCH(CH_3)CH_2NMe_2$, (b) $HOCH_2CH_2NMe_2$, (c) $HOC(CH_3)_2CH_2OMe$, and (d) $HOCH_2CH_2OMe$ at 550 °C.

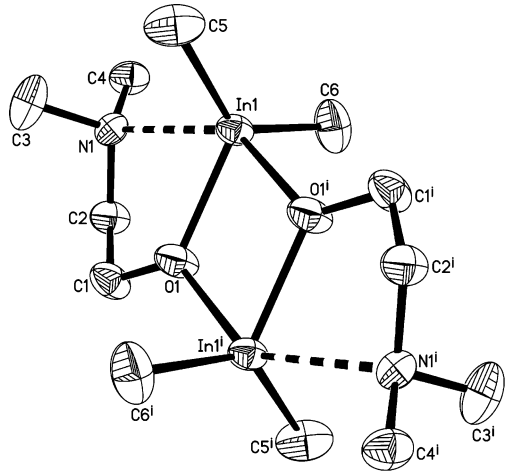

Figure 3. X-ray structure of $[Me_2In(OCH_2CH_2NMe_2)]_2$ (**1**) with thermal ellipsoids shown at the 50% probability level (hydrogen atoms omitted for clarity). Symmetry code: (i) $-x+1,-y+1,-z+1$.

complex,[36] is planar in **1**−**4**. Each indium atom in compounds **1**−**3** adopts a distorted trigonal bipyramidal geometry with two methyl groups in equatorial positions (Figures 3−5). The bridging alkoxide groups are located in both axial and equatorial positions, while the donor atom (L) of the alkoxide ligand (N for **1** and **2**; O for **3**) is in the axial position with the L−In−O bond angle to the opposite, axial alkoxide group ranging from 143.37(4)−146.99(4)°. This large deviation from 180° is due to the constraints of the internal O−In−O angle (range from 71.75(6)−74.17(5)°) in the In_2O_2 ring and the geometry of the ligand. The sum of the bond angles in the equatorial plane of **1**−**3** are close to 360°, which is a measure of the planarity of the equatorial groups. The equatorial In−O bond lengths in **1**−**3** are significantly shorter than the axial In−O bond distances (Table 3). The In−L distances in **1**−**3** range from 2.5161(16) to 2.5810(13) Å and can be attributed to L→In dative bonding. Compound **1** and related compounds, such as $[Me_2In(OC(CF_3)_2CH_2NHR)]_2$ (R = $(CH_2)_2OMe$), have been previously reported with comparable bond lengths and angles.[23,37,38]

The structure of compound **4** was determined by single-crystal X-ray crystallography, the results of which are shown in Figure 6; selected bond lengths and angles are given in Table 3. Compound **4** also exhibits a dimeric molecular arrangement similar to **1**−**3**, and the centrosymmetric, four-membered In_2O_2 ring is planar. However, each indium atom in **4** can be considered to be six-coordinate due to the presence of two donor (NMe_2) groups in the alkoxide ligand. As expected, the dative In−N bond lengths are long (In1−N1 2.8329(21) Å and In1−N2 2.9302(18) Å) but shorter than the sum of the van der Waals radii of In and N. The geometry of the indium atom in **4** can be considered as highly distorted octahedral. The distortions from ideal octahedral symmetry

(36) Schumann, H.; Kaufmann, J.; Wassermann, B. C.; Girgsdies, F.; Jaber, N.; Blum, J. *Z. Anorg. Allg. Chem.* **2002**, *628*, 971.
(37) Carmalt, C. J.; King, S. J. *Coord. Chem. Rev.* **2006**, *250*, 682.
(38) Hecht, E.; Gelbrich, T.; Thiele, K.-H.; Sieler, J. *Main Group Chem.* **2000**, *3*, 109.

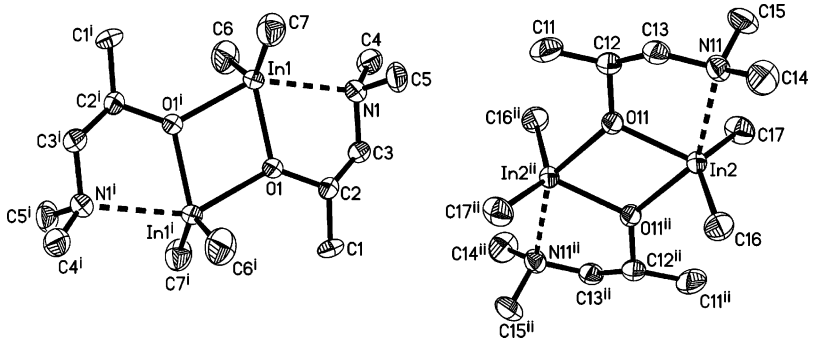

Figure 4. X-ray structure of $[Me_2In(OCH(CH_3)CH_2NMe_2)]_2$ (**2**) showing the two independent molecules with thermal ellipsoids shown at the 50% probability level (only the major component is shown and hydrogen atoms are omitted for clarity). Symmetry codes: (i) $-x+1,-y+2,-z$ and (ii) $-x+1,-y+1,-z+1$.

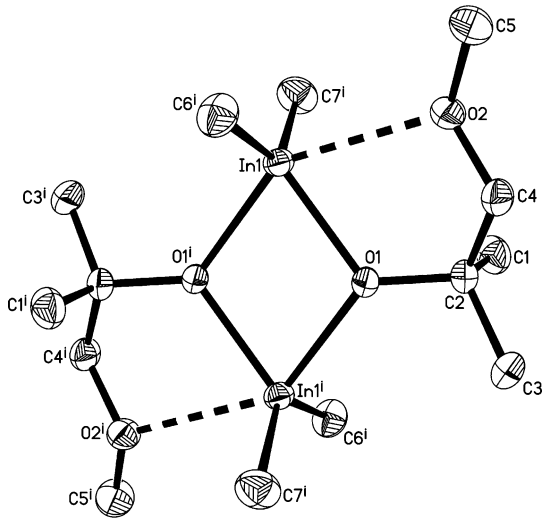

Figure 5. X-ray structure of $[Me_2In(OC(CH_3)_2CH_2OMe)]_2$ (**3**) with thermal ellipsoids shown at the 50% probability level (hydrogen atoms omitted for clarity). Symmetry code: (i) $-x+1,-y,-z+2$.

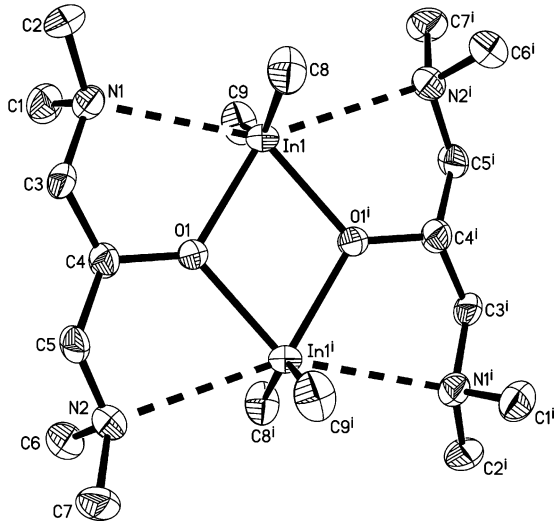

Figure 6. X-ray structure of $[Me_2In(OCH(CH_2NMe_2)_2]_2$ (**4**) with thermal ellipsoids shown at the 50% probability level (only the major component is shown and hydrogen atoms are omitted for clarity). Symmetry code: (i) $-x+1,-y,-z+1$.

observed in **4** are greater than the distortions found for **1**−**3**. The most significant deviations from octahedral geometry are found in the N1−In−N2 angle (150.82°) and N−In−O1 angles (av 68.21°), which are probably due to constraints imposed by the aminoalkoxide ligand. Significant deviations from octahedral geometry have been observed in other six-coordinate indium compounds.[36] Typically, distortions are observed due to constraints imposed by the ligands. In compound **4**, these would include a small O−In−O angle due to the In_2O_2 ring and the five-membered NInOCC rings.

Compounds **1**−**4** were prepared from the 1:1 reaction of Me_3In and ROH at room temperature. However, for the AACVD experiments, although the mixture was stirred at the same temperature, the proportions of Me_3In to ROH were 1:6. Solution-phase reactions between Me_3In and 6 equiv of ROH at room temperature have been carried out, but in all cases only dimethylindium alkoxides, $[Me_2InOR]_2$ (**1**−**4**), were isolated.[39] There was no evidence for the formation of indium bis(alkoxides) $[MeIn(OR)_2]_n$ or indium tris(alkoxides) $[In(OR)_3]_n$. These results are not surprising based on previous reports where attempts to transform metallanes, via the reaction of Me_3M and excess ROH, into bis(alkoxides), $[MeM(OR)_2]_n$, have failed and only afforded $[Me_2M(OR)]_n$.[40] We have previously shown that a 1:1 mixture of $[Et_2GaOR]_2$ and $[EtGa(OR)_2]$ could be obtained from the reaction of R_3Ga and excess ROH in refluxing toluene for 24 h.[24] Similar results have also been obtained from the reaction of Me_3In and excess ROH in refluxing toluene.[39] These results provide further evidence that the in situ AACVD reaction only resulted in the formation of the intermediate $[Me_2InOR]_2$. Further reaction of $[Me_2InOR]_2$ with excess alcohol to yield the indium bis(alkoxide) $[MeM(OR)_2]_n$ is unlikely since the AACVD bubbler is maintained at room temperature and not heated to the temperatures necessary for further methane elimination.

Conclusions

Thin films of In_2O_3 can be grown from Me_3In and ROH ($R = CH_2CH_2NMe_2$, $CH(CH_3)CH_2NMe_2$, $C(CH_3)_2CH_2OMe$, CH_2CH_2OMe) under AACVD conditions. This represents the first deposition of In_2O_3 by AACVD. Furthermore, the in situ reaction of Me_3In and ROH eliminates the need for the synthesis, isolation, and purification of a single-source indium alkoxide precursor. The 1:1 reaction of Me_3In and ROH resulted in the isolation of $[Me_2In(OR)]_2$, which have been structurally characterized. These reactions provide some

(39) Basharat, S. Ph.D. Thesis, University of London, 2007.
(40) Neumüller, B. *Chem. Soc. Rev.* **2003**, *32*, 50.

indication of compounds present (both solution phase and AACVD reactions were carried out in toluene at room temperature) in the AACVD flask prior to deposition.

Acknowledgment. EPSRC are thanked for a studentship (S.B.) and UCL MAPS faculty UCL for a research fund (C.J.C.). Dr. Geoff Hyett (UCL) is thanked for his help with XPS and Pilkington Glass for glass substrates.

Supporting Information Available: X-ray crystallographic data in CIF format for the structures of compounds **1**−**4**. This material is available free of charge via the Internet at http://pubs.acs.org.

IC701372B